RSC Advances

PAPER

View Article Online
View Journal | View Issue

Cite this: *RSC Adv.*, 2023, **13**, 19002

Facile preparation of high performance GO/Mn_3O_4/PVDF composite membranes with intercalation of manganese oxide nanowires

Han Runlin, *[a] Wang Chaoyue, [a] Bi Congcong[b] and Wang Hanli*[b]

Polyvinylidene fluoride (PVDF) has been widely studied and applied in separation membranes due to its high thermal and chemical stability and mechanical strength. However, PVDF has strong hydrophobicity, resulting in easy contamination of the membrane surface and fast flux attenuation, so it is necessary to modify the membrane surface to improve its separation selectivity and service life. In this paper, PVDF microporous membrane was used as the matrix material and graphene oxide (GO) as the separation layer material. The GO/Mn_3O_4/PVDF composite membrane was prepared by layer self-assembly of GO nanosheets, and the functional layer spacing was adjusted by nanometer Mn_3O_4 intercalation. The prepared composite membrane showed high flux and separation selectivity in the filtration of organic compounds. The results showed that the rejection of methylene blue increased from 34% to 99.5%, and the flux decreased from 3000 L m^{-2} h^{-1} to 95 L m^{-2} h^{-1} when GO nanosheets covered the PVDF supporting membrane. After the introduction of Mn_3O_4 nanowires in the GO interlayer, the dye rejection reached 99.9% and the flux reached 612 L m^{-2} h^{-1}. Compared with the unintercalated composite membranes, the flux of the prepared composite membranes showed good stability in the treatment of methylene blue, and the rejection remained unchanged.

Received 19th April 2023
Accepted 17th June 2023

DOI: 10.1039/d3ra02594b

rsc.li/rsc-advances

1. Introduction

Membrane separation technology showed a number of advantages such as environmentally friendly, simple operation, high treatment efficiency, small footprint, easy integration and so on. It has been widely studied and applied in desalination, wastewater treatment, medicine, energy and other fields. PVDF was widely used as the material for microfiltration, ultrafiltration, membrane distillation and membrane contactors, because of its excellent thermal stability, mechanical strength, and chemical resistance.[1] However, compared with other commercial polymer materials, PVDF has strong hydrophobicity, and the surface of the membrane is prone to serious pollution. It is also difficult to directly obtain the nanofiltration membrane with high flux and dense skin, which limits the application of PVDF membrane. In recent years, a lot of research work mainly focuses on the preparation of composite membranes or organic and inorganic hybrid membranes to adjust the properties of membranes.[2] Ashish Srivastava *et al.* reported that hexagonal boron nitride (h-BN) was used as inorganic nano-filler to prepare PVDF hybrid membranes, which helped water molecules transfer rapidly through nanochannels and reduced membrane pollution.[3] Prachi Awasthi *et al.* introduced boron nitride nanosheets (BNNSs) into PVDF membrane making solution, and prepared separation membranes by immersion precipitation phase conversion method, which can be used for simultaneous removal of tetracycline (TC) and ofloxacin (OFL).[4] Cao *et al.* investigated the effect of TiO_2 nanoparticle size on the structure and performance of PVDF membrane, and the results showed that smaller nanoparticle affected the hydrophilicity of the membrane significantly.[5] Due to the large number of carboxyl and hydroxyl groups on GO, it has a good affinity and is suitable for the preparation of organic and inorganic hybrid ultrafiltration membranes. Compared with undoped PVDF membranes, GO doped PVDF membranes showed stronger hydrophilicity and higher pure water flux. When 0.20 wt% GO was added in the casting solution, the performance and structure of the blend membrane were both improved obviously. The flux of the hybrid membrane increased by 96.4%, and the tensile strength increased by 123%. The anti-fouling performance of the hybrid membrane was also improved significantly.[6] Xu *et al.* prepared a novel Fe_3O_4/GO–PVDF hybrid ultrafiltration membrane with phase inversion technique assisted with magnetic field. The membranes exhibited significantly improved hydrophilicity and water flux because nanocomposites could migrate toward the membrane top surface due to magnetic function.[7] Wu *et al.* used aqueous solution of GO as the coagulation bath to prepare PVDF membrane with improved hydrophilicity.[8]

[a]*School of Chemistry and Chemical Engineering, Jinggangshan University, Ji'an 343009, China. E-mail: hanrunlin@163.com*

[b]*Shandong Huaxia Shenzhou New Material Co., Ltd., Zibo 256400, China*

Because GO is composed of a single layer of carbon atoms and has good mechanical properties, stacking the sheet structure of GO will form a layered membrane, which can rapidly improve the separation selectivity of PVDF membrane. Zhao *et al.* grafted GO tablets onto PVDF membrane by chemical activation and layer by layer self-assembly. The pore size of the modified membrane decreased significantly, and the surface electronegativity and hydrophilicity increased significantly. Due to the increased volume rejection effect, the retention rate of protein, humic acid and fulvic acid was improved.[9] Shi *et al.* prepared a novel photocatalytic membrane by vacuum assisted layer self-assembly of GO nanosheets and g-C_3N_4, then cross-linked with glutaraldehyde to construct a stable coating. The composite membrane showed higher permeability flux and higher separation selectivity for oil-in-water emulsion.[10] Unfortunately, GO composite membranes still faced deterioration of performance due to surface adsorption and pollutant deposition, and the small interlayer spacing resulted high mass transfer resistance. Therefore, it is urgent to improve the anti-pollution performance and stability of GO composite membranes.[11] Zhang *et al.* presented a highly stable and ultra-permeable zeolitic imidazolate framework-8 (ZIF-8)/GO membrane with a water permeability of 60 L m^{-2} h^{-1} at 0.1 MPa because ZIF-8 enlarged the interlayer spacing and produced a stable microstructure.[12] Wang *et al.* assembled GO nanosheets with polycation to form a multilayer composite membrane which showed enhanced stability and fouling resistance.[13]

Manganese oxide (MnO_x) was widely used in environmental purification because of advantages such as multiple valence of manganese, strong oxidation and adsorption capacity, high abundance, low toxicity, and high environmental compatibility. These unique properties make it a promising functional nanomaterial for the removal of organic pollutants. In our group, nanosized Mn_3O_4 nanowires were prepared with $KMnO_4$ and ethanol in mild conditions.[14] The prepared nanomaterials exhibited high activity in the treatment of phenol at acid condition and room temperature. The nanomaterials also showed high removal efficiency in dye treatment.[15] However, this material still fetters its further application due to high surface energy. Nano-sized Mn_3O_4 particles are prone to aggregation and deactivation in adsorption and catalytic process.[16] In addition, they tend to be suspended in water and require additional processes to recover the material, limiting their practical use in aqueous media to some extent. Therefore, it is necessary to develop a new membrane assembly process to reduce catalyst loss, increase catalyst load and improve membrane separation performance.[17,18]

In order to combine the advantages of membrane separation and catalytic reaction in single process, Mn_3O_4 nanowires were intercalated into the GO layers in this work. At the same time, Mn_3O_4 nanowires were used to regulate the GO layer spacing, improve the GO membrane compression resistance and pollution resistance. To improve the binding force between the nanosheets, manganese oxide and the supporting membrane, polydopamine (PDA) was formed during membrane preparation with self-polymerization of dopamine hydrochloride.[19] The composite membrane structure and morphology were tested with scanning electron microscope (SEM), X-ray photoelectron spectrometer (XPS) and atomic force microscope (AFM). This work studied the utility of nanomaterials intercalation technique to improve the performance of GO/PVDF composite membranes, providing a novel nanofiltration membrane with excellent permselectivity.

2. Experimental

2.1. Materials and instruments

Dopamine hydrochloride, $KMnO_4$, Na_2CO_3, methylene blue, methyl orange and rhodamine B are all analytically pure and obtained from Aladdin (Shanghai, China) without further purification. GO multilayer nanosheets (Tanfeng Tech Inc, China) were used as the functional layer material. PVDF was provided by Shandong Huaxia Shenzhou New Material Co., Ltd. PVDF membrane (0.22 μm, 47 mm) was provided by Yuling Filter Co., Ltd (Shanghai, China). Mn_3O_4 nanowires were prepared with hydrothermal method as shown in ref. 11. Vacuum pump (SCJ-10, Shupeilab, Shanghai, China) was used to prepare composite membrane. Constant temperature magnetic heating agitator (85-2, Jintan Honghua Instrument Factory, Jiangsu Province, China) and ultrasonic cleaners (KQ-50E, 40 kHz, Kunshan Ultrasonic Instrument CO., LTD, China) were used to obtain homogeneous solution.

2.2. Membrane preparation

The PVDF (M1) membrane without modification was used as control sample. The GO/PVDF (M2) and GO/Mn_3O_4/PVDF (M3) membranes were prepared *via* using vacuum-assisted self-assembly and cross-linked by dopamine. For the M2 membrane, the GO nanosheets solution was prepared with a concentration of 100 mg L^{-1} in a 200 mL water solution. Dopamine hydrochloride and $KMnO_4$ were also added with a concentration of 2 g L^{-1} and 0.2 g L^{-1}, respectively. The mixture was treated by sonication for 40 min, and directly vacuum-filtrated onto the PVDF membrane supports. As the filtrate flowed through, the composite membrane was formed. For the M3 composite membrane, GO and Mn_3O_4 were all fixed to 50 mg L^{-1}, respectively. Other steps are all the same for comparison.

2.3. Membrane characterization

The permeation performance of the composite membranes was evaluated by a dead-end membrane filtration system including nitrogen cylinder, membrane module, solution reservoir. The properties of the membrane such as flux (F) and rejection rate (R) are characterized by the setup. The concentration of organic compounds containing methylene blue was fixed at 50 mg L^{-1}. UV-vis spectrometer (721, Shanghai Youke, China) was used to detect the concentration of dye solution. The pure water flux and solute repulsion of the membrane were measured under the conditions of 0.1 MPa pressure and 20 °C. The permeation flux (F) was calculated as follows:

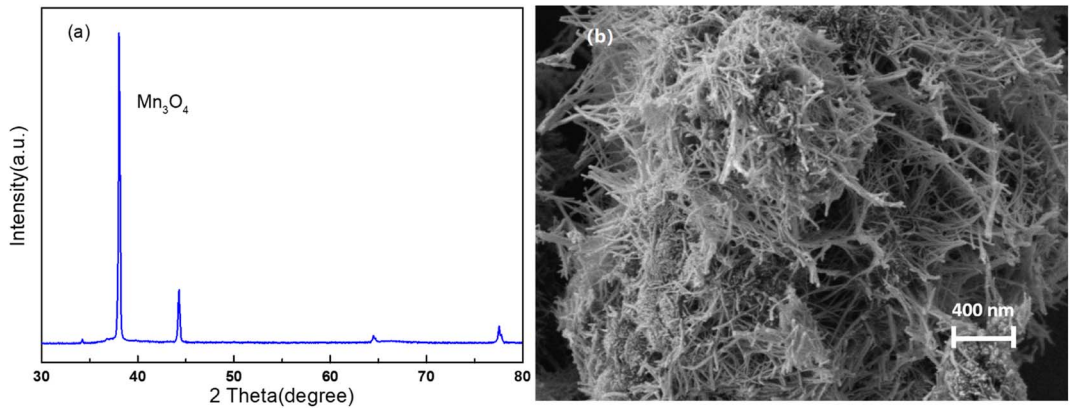

Fig. 1 Mn_3O_4 nanomaterials (a) XRD pattern, (b) SEM morphology.

$$F = \frac{W}{At} \quad (1)$$

where W is the total volume of the water or solution permeated during filtration process; A is the valid membrane area; and t is the operation time. Rejection, R, is calculated using the following equation:

$$R = \left(1 - \frac{C_p}{C_f}\right)\% \quad (2)$$

where C_p and C_f are the concentrations of the permeate solution and the feed solution, respectively. All the experiments on flux and rejection were repeated for three times.

The membranes were treated with gold spraying before scanning of SEM, and then tested with SEM (NovaSEM450, FEI, USA) with an acceleration voltage of 10 kV. At the same time, energy disperse spectroscopy (EDS) component was used for surface scanning and element content analysis. The morphology of the membrane was also tested with atomic force microscope (AFM, Bruker, Dimension ICON). The element composition of the material was analyzed by X-ray Photoelectron Spectrometer (XPS, ESCALAB 250Xi, Thermo Fisher). The contact angle of the membranes was characterized with Contact Angle Meter (CA100A, Shanghai Innuo Precision).

3. Results and discussion

3.1. Membrane characterization

The crystal phase and structure of the material were analyzed by XRD, and the XRD pattern was shown in Fig. 1a. The diffraction peaks of nanomaterial were consistent with the tetragonal Mn_3O_4 according to JCPDS no. 24-0734. No obvious impurity phase was detected. The morphology of the material was shown in Fig. 1b, where a lot of nanowires with uniform diameter were observed. The results demonstrated that Mn_3O_4 nanowires were successfully prepared by hydrothermal method, which can be used to prepare composite membrane.

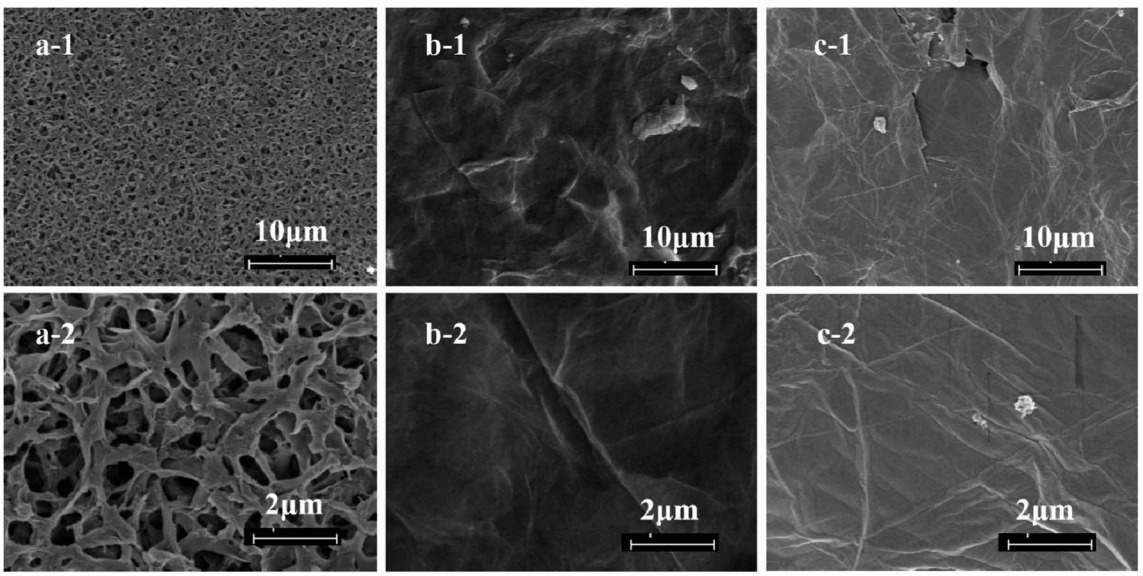

Fig. 2 Top surface SEM images of (a) M1 membrane, (b) M2 composite membrane and (c) M3 composite membrane.

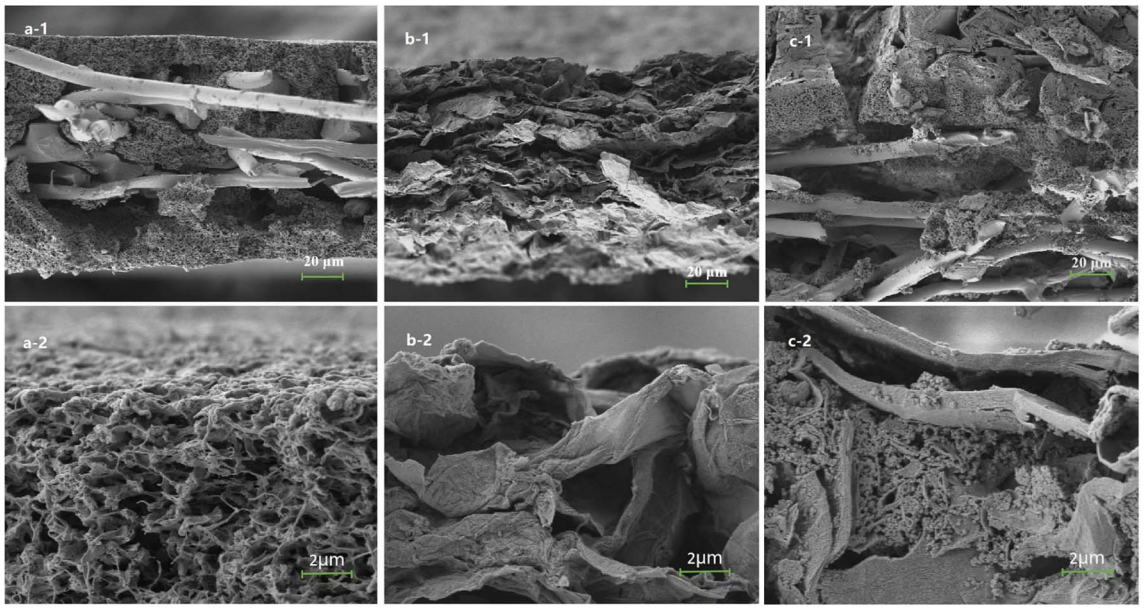

Fig. 3 Cross-section SEM images of (a) M1 membrane, (b) M2 composite membrane and (c) M3 composite membrane.

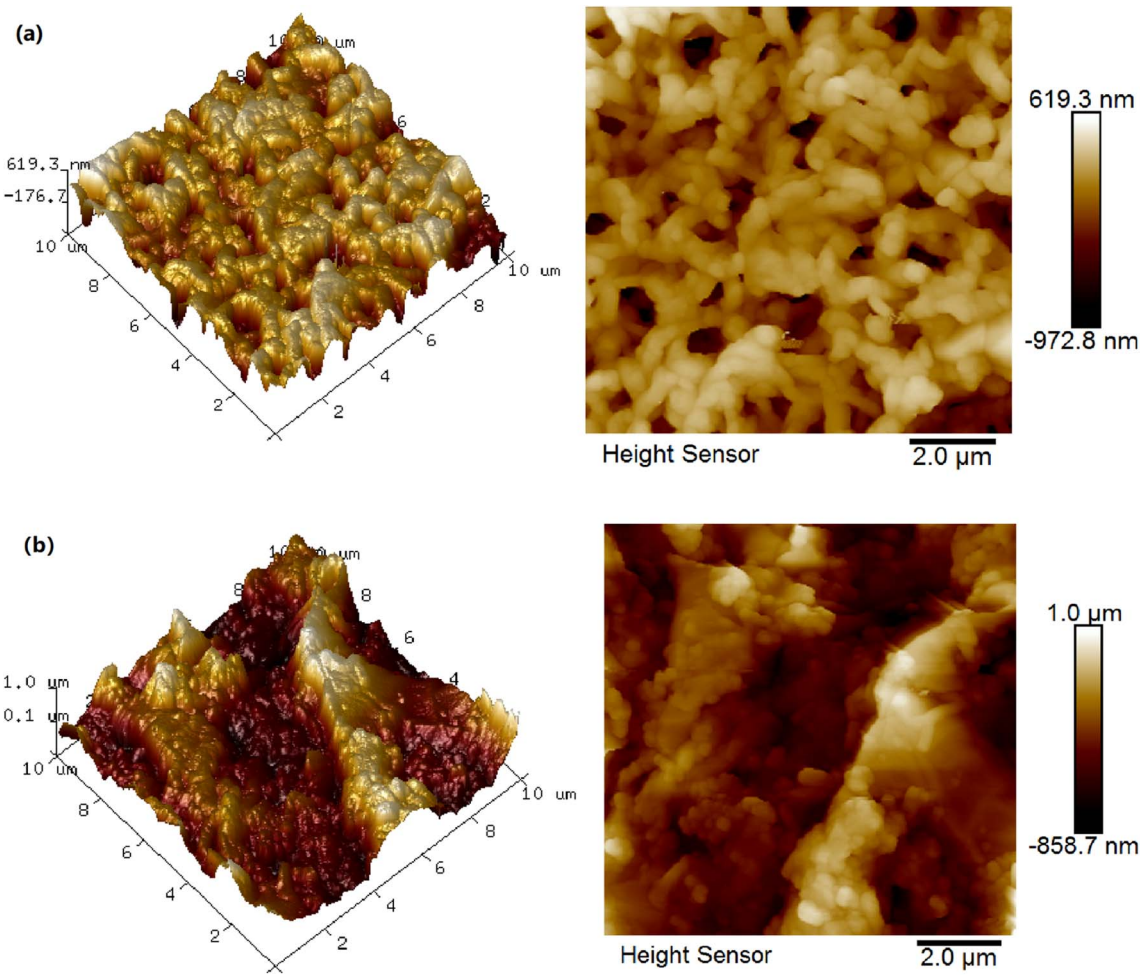

Fig. 4 AFM images of M1 and M3 membranes.

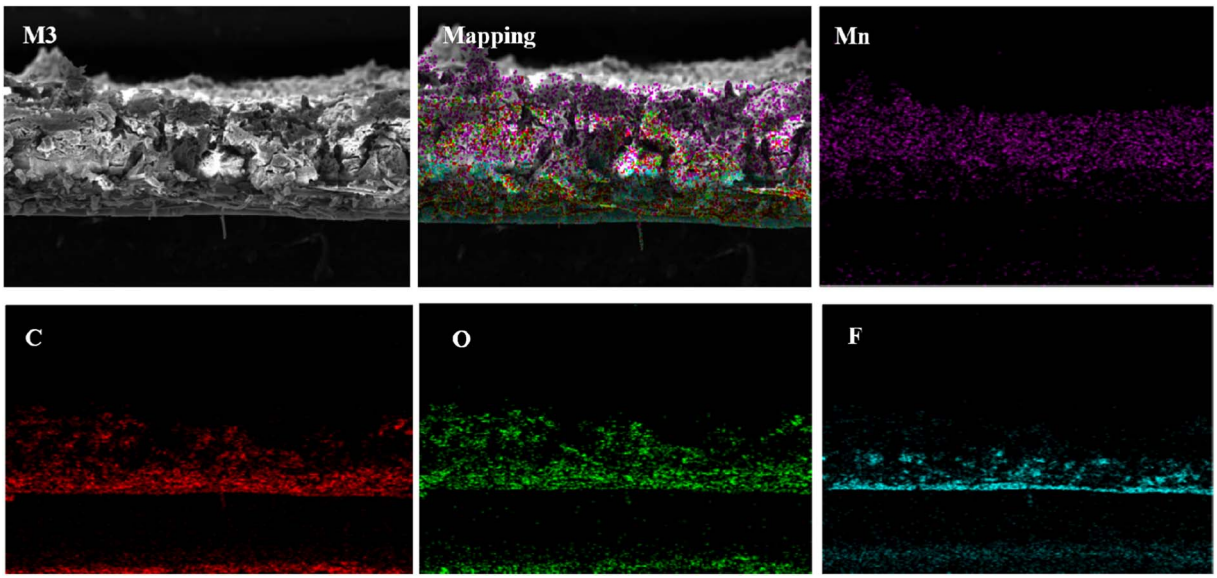

Fig. 5 Cross-section mapping of the M3 membrane.

As can be seen from the Fig. 2, the commercial PVDF membrane has a very uniform surface with a pore size of about 2 μm. The M1 membrane has very high porosity which is very helpful for mass transfer. In order to improve the separation accuracy of the PVDF membrane, the GO functional layer was introduced on the PVDF supporting membrane. As can be seen from the Fig. 2b, the surface of the composite membrane is very smooth, and the membrane holes are almost invisible. Very typical wrinkles of GO sheets can be observed in the membrane surface. When nano Mn_3O_4 nanowires were introduced into the GO interlayers, the surface of the membrane was still very dense and smooth, which endowed the membrane high selectivity.

The cross-section structure of the membrane was also analyzed and characterized by SEM as shown in Fig. 3. It can be seen from the Fig. 3a that the cross-section of PVDF supporting membrane is relatively uniform with a large number of pores. The polyester reinforced fibers were in the middle of the membrane. When GO functional layer was introduced, the typical graphene lamellar structure can be observed in Fig. 3b. The layer spacing was relatively small and the membrane was very dense. When Mn_3O_4 nanowires were intercalated in the GO layer, loose GO composite membrane was formed as shown in Fig. 3c, which has a significant effect on membrane flux enhancement. The high resolution images can give out the details of the membrane structure.

Fig. 4 showed the surface roughness of the supporting PVDF membrane and GO/Mn_3O_4/PVDF composite membrane which tested by AFM with a testing area of 10 μm × 10 μm. For the supporting membrane, uniform pores can be observed and the membrane has relative smooth surface with R_q (217 nm) and R_a (164 nm). The composite membrane showed rough surface and large protuberances with R_q (303 nm) and R_a (248 nm). The results were in accordance with the images of SEM. The GO membrane is often very smooth. In this work, the intercalated nanomaterials increased the roughness of the GO functional layer.

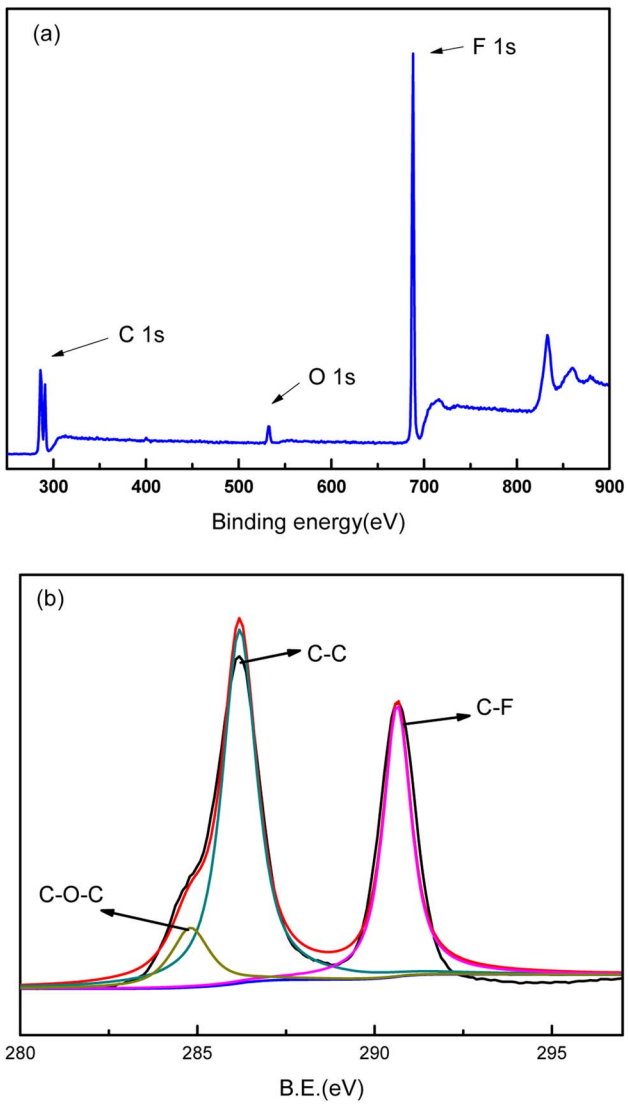

Fig. 6 XPS spectra of PVDF membrane. (a) Survey spectrum and (b) detailed spectrum of C 1s.

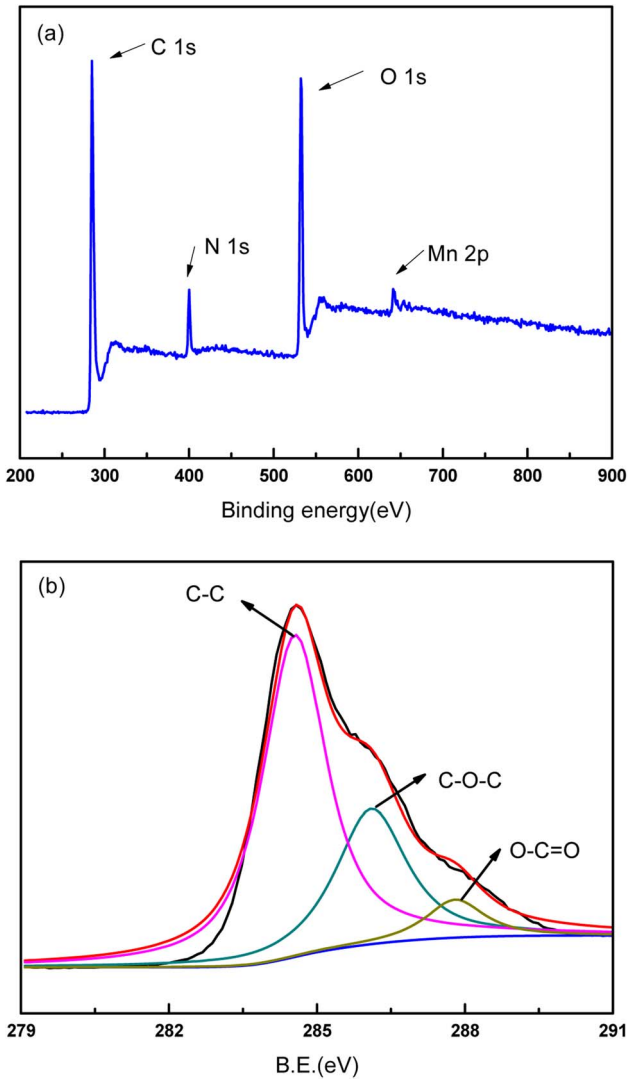

Fig. 7 XPS spectra of M2 composite membrane. (a) Survey spectrum and (b) detailed spectrum of C 1s.

In order to understand the structure and element composition of the composite membrane, the cross section of the membrane was analyzed by EDS mapping scanning. As shown in Fig. 5, Mn elements are mainly concentrated in the functional layer of the membrane and distributed evenly. Since the bottom layer is PVDF membrane, the F element is mainly concentrated in the position of supporting membrane. The C element is mainly derived from PVDF and GO, while the O element is derived from Mn_3O_4 and GO. And the polyester reinforced fibers in the PVDF membrane also contain C and oxygen. As can be seen from the figure, the high content of manganese oxide nanomaterials can widen the distance between the GO membranes, thus significantly increasing the membrane flux. At the same time, the introduced nanoparticles have high catalytic degradation activity, which is helpful to improve the anti-pollution performance of the membranes.

XPS analysis was conducted on the PVDF membrane and composite membranes to investigate the binding energy and

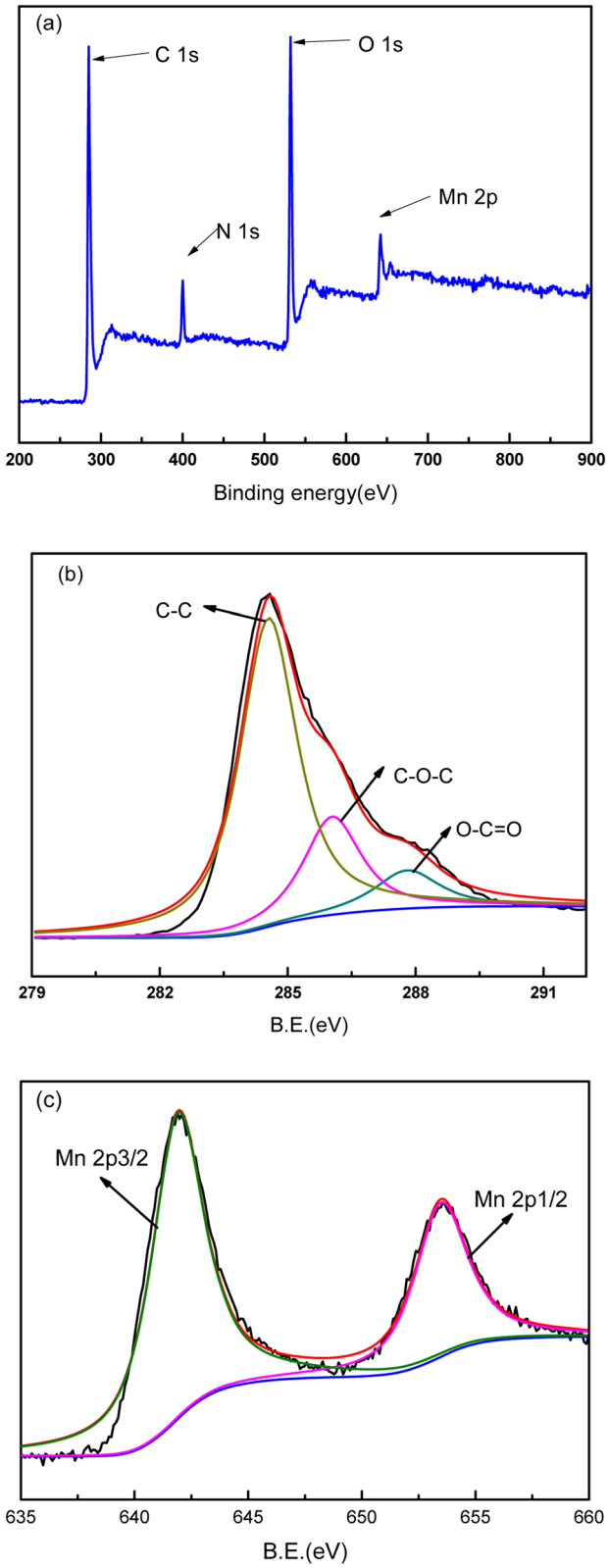

Fig. 8 XPS spectra of M3 composite membrane. (a) Survey spectrum, (b) detailed spectrum of C 1s and (c) detailed spectrum of Mn 2p.

composition of the samples (Fig. 6–8). As shown in Fig. 6, the major peaks were observed for PVDF, indexed as C 1s (286 eV and 290.8 eV), O 1s (534 eV), and F 1s (688 eV). The high-

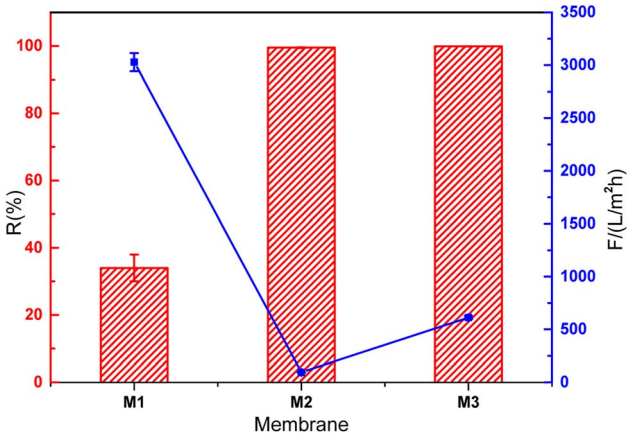

Fig. 9 Separation performance of the composite membranes.

resolution XPS spectrum for C element was presented in Fig. 6b. The sharp peaks located at 286 eV and 290.8 eV were attributed to C–C bond and C–F bond, respectively. Because of polyester fiber in the PVDF membrane, C–O–C bond also was detected in the high-resolution XPS spectrum of C 1s. The XPS spectra of GO/PVDF composite membrane were shown in Fig. 7. The major peaks located at 284.6 eV, 400 eV, 532 eV and 640 eV were attributed to C 1s, N 1s, O 1s, and Mn 2p, respectively. N was observed because PDA was formed in the functional layer with the polymerization of dopamine. Mn was also detected because $KMnO_4$ was used to accelerate the polymerization and MnO_2 nanoparticles were formed in the functional layer. Due to the large thickness of the GO functional layer, the probe of XPS did not detect the elements of the base membrane and no F 1s peak was detected. As shown in Fig. 7b, the high-resolution spectrum of C 1s was presented. The peaks located at 284.7 eV, 286 eV, and 287.9 eV were attributed to C–C bond, C–O–C bond, and C–O═C bond, respectively. The C element came mainly from GO and PDA in the functional layer. The XPS spectra of GO/Mn_3O_4/PVDF membrane were similar with the GO/PVDF membrane as shown in Fig. 8. The intensity of peak of Mn 2p was elevated because of intercalated nanoscale Mn_3O_4. In the high resolution Mn 2p XPS spectrum (Fig. 8c), the electron spin energy of Mn $2p_{3/2}$ and Mn $2p_{1/2}$ spectral peaks located at 641.3 eV, 642.8 eV and 653.3 eV, which indicated the coexistence of Mn^{4+} and Mn^{3+}.

3.2. Separation performance of the composite membranes

Separation performance of the composite membranes was shown in Fig. 9. PVDF support membrane has large pore size and porosity, so its permeability flux reached about 3000 L m^{-2} h^{-1}, but its methylene blue rejection is only 34%. When the GO functional layer was introduced into the PVDF support membrane, the permeability of the membrane decreased significantly, only 95 L m^{-2} h^{-1}. Because of the small GO membrane spacing, the dye rejection increased greatly from 34% to 99.5%. When the Mn_3O_4 nanoparticles were inserted into the GO interlayer, the dye rejection of the membrane was slightly improved from 99.5% to 99.9%, and the flux of the

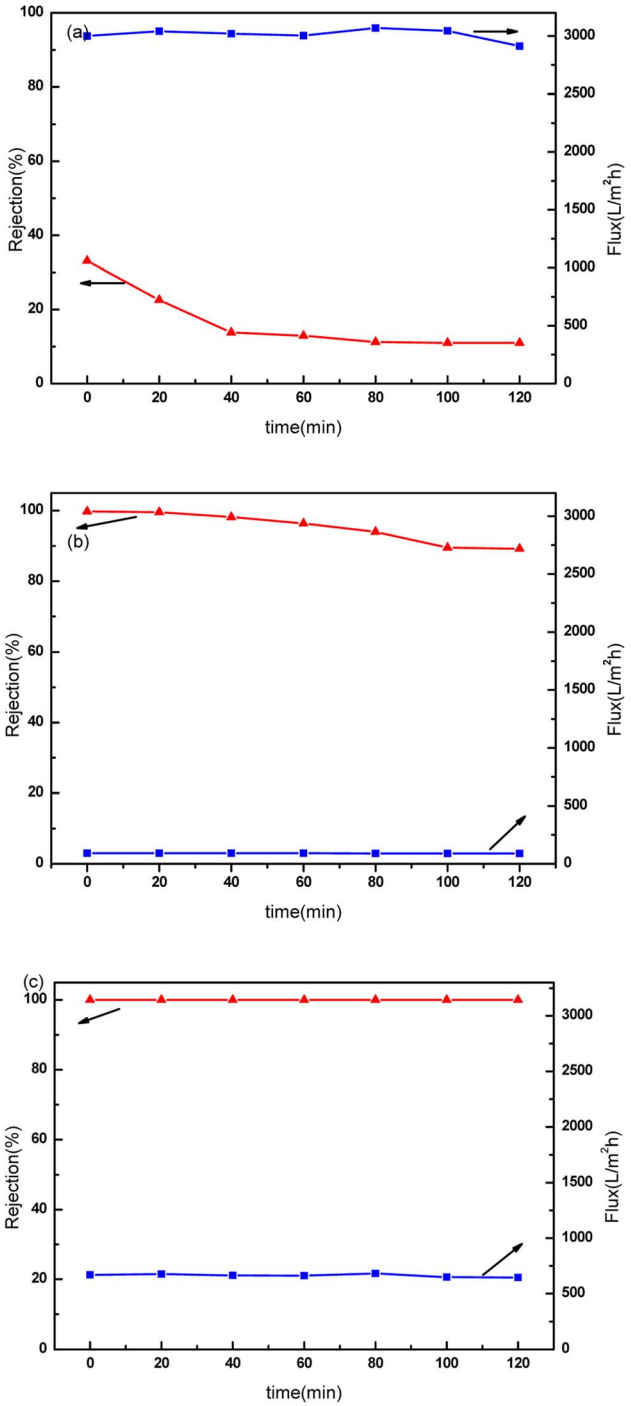

Fig. 10 Fouling resistance of the composite membranes. (a) M1 membrane, (b) M2 composite membrane, (c) M3 composite membrane.

Table 1 The performance of the M3 composite membrane

Feed	Methyl orange	Rhodamine B	Tetracycline hydrochloride
MW (Da)	327	480	481
F (L m^{-2} h^{-1})	768	840	718
R (%)	64.2	99.3	89.3

Table 2 Comparison of membrane performance

Membrane material	Permeate	Rejection (%)	Flux (L m^{-2} h^{-1})	Pressure (MPa)	References
Fe_3O_4/GO–PVDF	Bovine serum albumin	92	595	0.1	7
PVDF–GB	Bovine serum albumin	67.6	467.8	0.1	8
ZIF-8/GO	Methylene blue	99	60	0.1	12
Polycation/GO	Methylene blue	99.2	6.42	0.1	13
Mn_3O_4/GO	Methylene blue	99.9	612	0.1	This work

membrane increased rapidly from 95 L m^{-2} h^{-1} to 612 L m^{-2} h^{-1}. The inserted nanoparticles significantly increased the layer spacing of GO functional layer and reduced the mass transfer resistance, so the flux of the membrane was rapidly increased. Moreover, the Mn_3O_4 nanoparticles have strong oxidation activity, and the methylene blue that penetrated into the membrane pore was degraded, so dye molecules were almost undetectable through the penetrant.

3.3. Fouling resistance of the composite membranes

The antifouling performance of PVDF membrane and composite membranes were tested with methylene blue solution as shown in Fig. 10. It was found that the flux of PVDF membrane decreased from 3000 L m^{-2} h^{-1} to 2911 L m^{-2} h^{-1}, while the dye rejection decreased from 33% to 11% during 120 min operation. With the extension of operation time, the membrane surface pollution was aggravated. The concentration polarization became more serious, and more dye molecules could penetrate PVDF membrane. So the separation selectivity of the membrane decreased. The GO/PVDF composite membrane showed dense functional layer. The dye rejection decreased from 99.8% to 89.2% within 120 min. After 60 minutes of operation, the decrease of rejection was more obvious, indicating that the GO membrane was swollen and the GO layer spacing was slightly increased. When Mn_3O_4 nanomaterials were introduced into the GO interlayer, the composite membrane showed 99.9% rejection to dye. And the membrane flux declined from 669 L m^{-2} h^{-1} to 645 L m^{-2} h^{-1}. The intercalated Mn_3O_4 can enhance the membrane flux obviously. The membrane showed excellent anti-fouling resistance because the intercalated nanomaterials can degrade methylene blue efficiently, and the membrane surface was not prone to contamination. The hydrophilicity of the membranes was also characterized with contact angle analysis after the drops stabilized for 5 s. The PVDF support membrane showed a contact angle of 74° because of the hydrophobicity of membrane materials. The M2 and M3 composite membranes showed improved hydrophilicity with the contact angles of 49° and 48°, respectively. The composite membranes showed excellent hydrophilicity because of the abundant of carboxyl and hydroxyl groups of GO nanosheets.

3.4. Comparison of membrane versatility and properties

The versatility of M3 composite membrane also was evaluated with other organic compounds such as methyl orange, rhodamine B and tetracycline hydrochloride at neutral condition and room temperature. Because of the dense functional layer and large interlayer spacing, the composite membrane possessed high rejection to organic molecules. The intercalated nanomaterials also can degrade organics and improve the rejection and flux of the membrane simultaneously. As shown in Table 1, the composite membrane showed high rejection (99.3%) to rhodamine B with high flux (840 L m^{-2} h^{-1}). Because of low molecular weight and linear molecular structure, rejection to methyl orange was relatively low (64.2%). The membrane also showed high rejection (89.3%) and flux (718 L m^{-2} h^{-1}) of tetracycline hydrochloride, which exhibited great potential in antibiotic wastewater treatment.

As shown in Table 2, the PVDF membrane modified with nanomaterials such as GO showed high water flux. The membranes showed relative high rejection to bovine serum albumin (66 kDa) which confirmed the character of ultrafiltration membrane. The GO composite membranes modified with ZIF-8 or polycation showed high rejection to methylene blue (320 Da) which can be classified as nanofiltration membrane. However, the membrane flux was not high enough. The composite membrane prepared in this work showed higher rejection and water flux compared with the performance data of other references. Because the nano-sized manganese oxide with excellent hydrophilic and oxidizing activity was intercalated into the GO layer, the membrane spacing was also stably controlled. So the composite membrane showed extremely high separation selectivity.

4. Conclusions

GO/Mn_3O_4/PVDF composite membrane was successfully prepared with a facile layer self-assembly of GO nanosheets and intercalated with Mn_3O_4 nanowires. The top surface of the composite membranes was very smooth without visible pores according to SEM images. EDS mapping of the cross-section membrane demonstrated the intercalation of Mn_3O_4 nanoparticles in the GO interlayer. XPS scanning also demonstrated the dense GO layer was formed on the PVDF membrane and Mn_3O_4 was intercalated successfully. The functional layer spacing was enlarged by nanometer Mn_3O_4 intercalation significantly, and the prepared composite membrane showed high flux and separation selectivity. The results showed that the dye rejection increased from 99.5% to 99.9% and the flux increased from 95 L m^{-2} h^{-1} to 612 L m^{-2} h^{-1}. The composite membrane also showed excellent fouling resistance during

120 min operation. The rejection of methylene blue did not decline while the flux kept stable because of the high oxidation and adsorption ability of the nanomaterials. The composite membranes showed good versatility, with high selectivity and flux in the separation of various organic compounds such as dyes and tetracycline hydrochloride.

Conflicts of interest

The authors declare no conflict of interest.

Acknowledgements

This research was funded by Jiangxi Province Double Thousand Talents Plan, grant number jxsq2020101049, Science & Technology Program of Jiangxi Provincial Education Bureau, grant number GJJ2201623, China Postdoctoral Science Foundation, grant number 2021M691964.

References

1 F. Liu, N. A. Hashim, Y. Liu, M. R. M. Abed and K. Li, Progress in the production and modification of PVDF membranes, *J. Membr. Sci.*, 2011, **375**, 1–27.

2 J. R. Du, S. Peldszus, P. M. Huck and X. Feng, Modification of poly(vinylidene fluoride) ultrafiltration membranes with poly(vinyl alcohol) for fouling control in drinking water treatment, *Water Res.*, 2009, **43**(18), 4559–4568.

3 A. Srivastava and Z. V. P. Murthy, Investigating the effect of PEG200 and two-dimensional h-BN on PVDF membrane performance for membrane distillation-crystallization, *Mater. Today Chem.*, 2021, **22**, 100545.

4 P. Awasthi, R. S. Bangari and N. Sinha, PVDF/BNNSs nanocomposite membrane for simultaneous removal of tetracycline and ofloxacin from water, *J. Mol. Liq.*, 2023, **370**, 120970.

5 X. Cao, J. Ma, X. Shi and Z. Ren, Effect of TiO_2 nanoparticle size on the performance of PVDF membrane, *Appl. Surf. Sci.*, 2006, **253**, 2003–2010.

6 Z. Wang, H. Yu, J. Xia, F. Zhang, F. Li, Y. Xia and Y. Li, Novel GO-blended PVDF ultrafiltration membranes, *Desalination*, 2012, **299**, 50–54.

7 Z. W. Xu, T. F. Wu, J. Shi, W. Wang, K. Y. Teng, X. M. Qian, M. J. Shan, H. Deng, X. Tian, C. Y. Li and F. Y. Li, Manipulating migration behavior of magnetic graphene oxide via magnetic field induced casting and phase separation towards high-performance hybrid ultrafiltration membranes, *ACS Appl. Mater. Interfaces*, 2016, **8**, 18418–18429.

8 T. F. Wu, B. M. Zhou, T. Zhu, J. Shi, Z. W. Xu, C. S. Hu and J. J. Wang, Facile and low-cost approach towards PVDF ultrafiltration membrane with enhanced hydrophilicity and antifouling performance via graphene oxide/water-bath coagulation, *RSC Adv.*, 2015, **5**, 7880–7889.

9 J. Zhao, Y. Yang, C. Li and L. Hou, Fabrication of GO modified PVDF membrane for dissolved organic matter removal: removal mechanism and antifouling property, *Sep. Purif. Technol.*, 2019, **209**, 482–490.

10 Y. Shi, J. Huang, G. Zeng, W. Cheng, J. Hu, L. Shi and K. Yi, Evaluation of self-cleaning performance of the modified g-C_3N_4 and GO based PVDF membrane toward oil-in-water separation under visible-light, *Chemosphere*, 2019, **230**, 40–50.

11 F. Li, Z. Yu, H. Shi, Q. Yang, Q. Chen, Y. Pan, *et al.*, A mussel-inspired method to fabricate reduced graphene oxide/g-C_3N_4 composites membranes for catalytic decomposition and oil-in-water emulsion separation, *Chem. Eng. J.*, 2017, **322**, 33–45.

12 W.-H. Zhang, M.-J. Yin, Q. Zhao, C.-G. Jin, N. Wang, S. Ji, C. L. Ritt, M. Elimelech and Q.-F. An, Graphene oxide membranes with stable porous structure for ultrafast water transport, *Nat. Nanotechnol.*, 2021, **16**, 337–343.

13 L. Wang, N. Wang, J. Li, J. Li, W. Bian and S. Ji, Layer-by-layer self-assembly of polycation/GO nanofiltration membrane with enhanced stability and fouling resistance, *Sep. Purif. Technol.*, 2016, **160**, 123–131.

14 R. Han, M. Chen, X. Liu, Y. Zhang, Y. Xie and Y. Sui, Controllable synthesis of Mn_3O_4 nanowires and application in the treatment of phenol at room temperature, *Nanomaterials*, 2020, **10**, 1–9.

15 R. Han, Y. Zhang and Y. Xie, Application of Mn_3O_4 nanowires in the dye waste water treatment at room temperature, *Sep. Purif. Technol.*, 2020, **234**, 116119.

16 R. Yang, Y. Fan, R. Ye, Y. Tang, X. Cao, Z. Yin and Z. Zeng, MnO_2-Based Materials for Environmental Applications, *Adv. Mater.*, 2021, **1**, 1–53.

17 M. Park, Y. T. Ko, M. Ji, J. S. Cho and D. H. Wang, Young-In Lee, Facile self-assembly-based fabrication of a polyvinylidene fluoride nanofiber membrane with immobilized titanium dioxide nanoparticles for dye wastewater treatment, *J. Clean. Prod.*, 2022, **378**, 134506.

18 V. Smuleac, L. Bachas and D. Bhattacharyya, Aqueous-phase synthesis of PAA in PVDF membrane pores for nanoparticle synthesis and dichlorobiphenyl degradation, *J. Membr. Sci.*, 2010, **346**, 310–317.

19 C. Wang, H. Wu, G. Yu, H. Zha and R. Han, Fast preparation of a polydopamine/ceramic composite nanofiltration membrane with excellent permselectivity, *RSC Adv.*, 2023, **13**, 615.